Journal of Physics: Condensed Matter

PAPER

OPEN ACCESS

RECEIVED
15 January 2026

REVISED
25 February 2026

ACCEPTED FOR PUBLICATION
6 March 2026

PUBLISHED
18 March 2026

Short-range order and atomic dynamics of $Ti_{75}Ni_{25}$ melts

Johanna Wilden[1], Dirk Holland-Moritz[1,*], Fan Yang[1], Nico Neuber[2], Ralf Busch[2], Thomas Voigtmann[1], Thomas C Hansen[3], Thomas Buslaps[4] and Andreas Meyer[1,3]

[1] Institute for Frontier Materials on Earth and in Space, German Aerospace Center (DLR), 51147 Köln, Germany
[2] Lehrstuhl für metallische Werkstoffe, Universität des Saarlandes, 66123 Saarbrücken, Germany
[3] Institut Laue-Langevin (ILL), 38042 Grenoble, France
[4] European Synchrotron Radiation Facility (ESRF), 38000 Grenoble, France
[*] Author to whom any correspondence should be addressed.

E-mail: dirk.holland-moritz@dlr.de

Keywords: short-range order of liquids, atomic dynamics, neutron diffraction, x-ray diffraction

Abstract

Preceding investigations on the atomic dynamics in melts of $Ti_{75}Ni_{25}$ revealed faster atomic dynamics as compared to that found in melts of $Zr_{64}Ni_{36}$ and $Ni_{66.7}B_{33.3}$, despite the fact that all these melts are characterized by similar packing fractions. In order to find a structural explanation for the different dynamic behavior, we have studied the short-range structure of stable and undercooled $Ti_{75}Ni_{25}$ melts. The melts were containerlessly processed under high-purity conditions by application of the electrostatic levitation technique. Partial structure factors of the liquid alloys have been determined by a combination of neutron diffraction (with isotopic substitution) and synchrotron x-ray diffraction. The studies reveal that $Ti_{75}Ni_{25}$ melts are characterized by a chemical short-range order, where heterogeneous Ti-Ni nearest neighbors are preferentially formed. This chemical short-range order, however, is less pronounced than the chemical short-range order reported for melts of $Zr_{64}Ni_{36}$ and $Ni_{66.7}B_{33.3}$. The less pronounced chemical short-range order may account for the faster atomic dynamics reported for liquid $Ti_{75}Ni_{25}$. For a further analysis of the structure-dynamics relationship the experimentally determined partial structure factors were used as an input for calculations in the framework of the mode coupling theory (MCT) of the glass transition. These reveal that the Ni self-diffusion is only slightly faster than the Ti self-diffusion with a ratio of the self-diffusion coefficients $D_{Ni}/D_{Ti} \approx 1.2$. Moreover, the Onsager coefficients calculated by MCT are in good agreement with those estimated by use of Darken's equation indicating that cross-correlation effects are negligible when describing the interdiffusion in liquid $Ti_{75}Ni_{25}$.

1. Introduction

The short-range structure and the atomic dynamics of melts are atomic scale properties that determine the macroscopic properties (such as density, viscosity, surface tension, or electrical resistivity) of the liquids and govern the solidification behavior. During solidification, the short-range order of the liquid determines the energy of the interface between the liquid phase and nuclei of the crystallizing solid phases, which is an important parameter that influences the crystal-nucleation from undercooled liquids [1–3]. The atomic dynamics influence both, crystal nucleation, and subsequent crystal growth [2–4]. Because glassy solids may be formed from undercooled liquids, if the crystallization of the melt is avoided, short-range order and atomic dynamics are key properties to find a microscopic understanding of the mechanisms underlying glass-formation. Apart from the decisive importance of both atomic scale properties for solidification and glass-formation in undercooled liquids, the relation between short-range structure and atomic dynamics is of fundamental scientific interest. One possibility to directly link the structure and the atomic dynamics of melts is provided by the mode coupling theory (MCT) of the glass transition [5, 6]. It allows to make predictions on dynamical quantities of the liquid, like self-diffusion

coefficients and viscosity, using partial static structure factors and densities of packing of the liquids as the only input parameters.

One metallic alloy system, which has been subject to a large number of experimental studies on the short-range structure and the atomic dynamics is Zr–Ni [7–11]. Using the experimentally determined partial structure factors, MCT predicts nearly identical Ni and Zr self-diffusion coefficients for Zr-rich $Zr_{64}Ni_{36}$ alloy melts, which means that the self-diffusion of Zr and Ni is strongly coupled [8, 10]. For $Zr_{64}Ni_{36}$, the Onsager coefficient is considerably lower than predicted by Darken's equation, which means that this equation is not valid here and that cross-correlation terms need to be considered [8]. The prediction by MCT of similar Zr and Ni self-diffusion coefficients, as well as the interdiffusion coefficients have been experimentally confirmed by tracer [9] and interdiffusion [11] measurements. It can be shown for $Zr_{64}Ni_{36}$ that this is a result of the structurally preferred Zr–Ni nearest-neighbor pairs, and a dominant, slow kinetic contribution to the interdiffusion. While for the Zr-rich $Zr_{64}Ni_{36}$ alloys strong coupling of the Ni and Zr self-diffusion is observed, increasing of the Ni composition results in a decoupling of the Ni and Zr self-diffusion, such that the Ni self-diffusion coefficient is roughly twice as large as the Zr self-diffusion coefficient for Ni-rich $Zr_{36}Ni_{64}$ melts [10]. The composition dependence of the coupling behavior as well as the temperature dependence of the Ni self-diffusivity in $Zr_{50}Ni_{50}$ is well reproduced by MCT with experimentally determined partial structure factors as an input [10]. This is also the case for melts of $Hf_{35}Ni_{65}$, where, similar as for $Zr_{36}Ni_{64}$, decoupled Ni and Hf diffusion is observed [12]. The decoupling of the diffusion coefficients for the Ni-rich alloys may be explained by a saturation of the fraction of strongly interacting Zr/Hf-Ni nearest neighbor pairs as suggested by an analysis of the experimentally determined partial coordination numbers [10, 12].

Recently, the structure [13] and the atomic dynamics [14] in melts of $Ni_{66.7}B_{33.3}$ has been studied. Despite the fact that B is a nonmetallic constituent with a considerably smaller atomic size than Ni, $Ni_{66.7}B_{33.3}$ shows almost identical Ni self-diffusion coefficients and melt viscosities as $Zr_{64}Ni_{36}$ at same temperature [14] (for the diffusivities see also figure 5). Using experimentally determined partial structure factors as an input, MCT delivers Ni self-diffusion coefficients and interdiffusion coefficients that are in good agreement with experimental results [13]. Different from $Zr_{64}Ni_{36}$, for $Ni_{66.7}B_{33.3}$ the MCT calculations suggest decoupled dynamics of the constituents (B diffuses roughly twice as fast as Ni) and that the interdiffusion is well described by Darken's equation [13].

Recent measurements of the density of molten $Ti_{75}Ni_{25}$ [15] revealed a similar packing fraction as reported for $Zr_{64}Ni_{36}$ [16]. Moreover, both early transition metals belong to the same group in the periodic table of the elements. Nevertheless, a higher mean Ti/Ni self-diffusion coefficient and a lower viscosity are found for $Ti_{75}Ni_{25}$ as compared to the Ni self-diffusivity and viscosity in $Zr_{64}Ni_{36}$ at same temperatures [15] (for the diffusivities see also figure 5). Even lower viscosities as found for $Ti_{75}Ni_{25}$ are reported for Ti-rich Ti–Cu alloys [17].

In this work we present investigations of the short-range structure of stable and undercooled $Ti_{75}Ni_{25}$ melts aiming to analyze the structure-dynamics relationship. In order to analyze the short-range order in a binary *A*–*B* melt, partial static structure factors may be calculated from three independent total static structure factors in the framework of the Bhatia–Thornton [18] or the Faber-Ziman formalism [19]. Bhatia and Thornton have defined three partial static structure factors: $S_{NN}(q)$, $S_{CC}(q)$, and $S_{NC}(q)$. $S_{NN}(q)$ describes the topological short-range order of the system, $S_{CC}(q)$ the chemical short-range order, and $S_{NC}(q)$ the correlation of number density and chemical composition. For neutron diffraction the relation between the total structure factors and the partial structure factors is given by:

$$S(q)^{\mathrm{BT}} = \frac{\bar{b}^2}{\overline{b^2}} S_{\mathrm{NN}}(q) + \frac{c_A c_B (b_A - b_B)^2}{\overline{b^2}} S_{\mathrm{CC}}(q) + \frac{2(b_A - b_B)\bar{b}}{\overline{b^2}} S_{\mathrm{NC}}(q). \tag{1}$$

Here c_A and c_B denote the concentrations of the atoms of type A and B in the melt, b_A and b_B are the coherent neutron scattering lengths of the atoms/isotopes, $\bar{b} = c_A b_A + c_B b_B$ and $\overline{b^2} = c_A {b_A}^2 + c_B {b_B}^2$.

Within the Faber-Ziman formalism the three partial static structure factors $S_{AA}(q)$, $S_{BB}(q)$, and $S_{AB}(q)$ describe the contributions to the total structure factor $S(q)$ that result from correlations between the three different types of atomic pairs (*A*–*A*, *B*–*B*, and *A*–*B*):

$$S(q)^{\mathrm{FZ}} = \frac{c_A^2 {b_A}^2}{\overline{b^2}} S_{AA}(q) + \frac{{c_B}^2 {b_B}^2}{\overline{b^2}} S_{BB}(q) + \frac{2 c_A c_B b_A b_B}{\overline{b^2}} S_{AB}(q) + 1 - \frac{\bar{b}^2}{\overline{b^2}}. \tag{2}$$

For x-ray diffraction similar equations apply, where the neutron scattering lengths b_A and b_B are replaced by the atomic x-ray scattering factors $f_A(q)$ and $f_B(q)$ of the different types of atoms. In order to determine all three Bhatia–Thornton or Faber-Ziman structure factors of a binary alloy three diffraction experiments must be performed under different scattering contrast conditions. In this work the variation

of the scattering contrast was done by a combination of neutron diffraction (with isotopic substitution) and synchrotron x-ray diffraction.

In order to gain deeper insight into the structure-dynamics relationship the experimentally determined partial structure factors are used as an input for MCT calculations. This provides information on the ratio of the self-diffusion coefficients and on the validity of Darken's equation.

2. Experimental

$Ti_{75}Ni_{25}$ master alloys, were produced from the pure elements/isotopes in a Ti-gettered arc furnace under an Ar atmosphere of 99.9999% purity. Pieces from the master alloy were remelted in the arc furnace, to obtain smaller spherical samples for electrostatic levitation. For the x-ray diffraction experiments sample masses between 100–150 mg were used, whereas for the neutron diffraction experiments sample masses between 400–600 mg were used, respectively.

Because of the high chemical reactivity of the Ti-based samples and in order to access also the metastable regime of an undercooled melt, for all diffraction studies the samples were containerlessly processed under high vacuum conditions at total pressures smaller than $1{\cdot}10^{-6}$ mbar in an electrostatic levitation furnace specially developed to perform neutron- or synchrotron scattering experiments [20]. The lack of crucible material in the vicinity of the levitating sample gives the extra advantage of an excellent signal to background ratio in scattering experiments. The temperature of the samples is contactlessly measured with an accuracy of ± 5 K using a single-color pyrometer that was calibrated such that the eutectic temperature visible in the temperature-time profiles corresponds to the literature value of $T_e = 1215$ K [21]. Please note that the liquidus temperature of $T_L = 1225$ K [21] is only 10 K above T_e, but less clearly visible in the temperature-time profiles than T_e. A detailed description of the ESL apparatus is given in [20].

Elastic neutron scattering experiments [22] on the short-range order were performed at the Institut Laue-Langevin in Grenoble, France, on the high-intensity two-axis diffractometer D20 [23] using a wavelength of the incident neutrons of $\lambda = 0.9434$ Å. The exact wavelength and the angular offset of the detector were determined from the diffractogram of a W standard. The static structure factors of the liquids, $S(q)$, as function of the momentum transfer, q, have been determined from the measured raw diffractograms by application of the same data evaluation procedure as described in [24], which includes background subtraction, correction of self-absorption, multiple scattering and of the effect of inelastic scattering and a normalization using a vanadium measurement. In order to vary the scattering contrast, the Ti–Ni samples were prepared with the Ni isotopes ^{60}Ni, ^{58}Ni as well as with Ni of natural isotopic abundance.

The synchrotron x-ray diffraction experiments were performed on the material science beamline ID11[25], located at the European Synchrotron Radiation Facility in Grenoble, France. The experiments were drawn out in transmission geometry with radiation of 0.12398 Å wavelength, which corresponds to an energy of 100 keV. The diffracted x-ray photons were detected by a FReLoN 2 K flat panel detector [26]. A range of momentum transfer between 0.2–16 $Å^{-1}$ was covered. The exposure time for each diffraction pattern was 0.5 s, whereas the total time between two diffraction pattern was 0.7 s. To calibrate the sample-to-detector distance, a CeO_2 standard was measured. With the azimuthal integration procedure provided by the pyFAI software [27], the 2-dimensional diffraction pattern was converted into 1-dimensional diffractograms $I(q)$. In this step, we performed dark current-, flat field-, and solid angle-corrections. From $I(q)$ the total static structure factors, $S(q)$, are calculated after subtraction of the background measured with the empty levitator, and correcting for self-absorption, Compton scattering, multiple scattering, polarization, and oblique incidence by using the PDFget2X [28] software.

3. Results and discussion

In order to determine the partial structure factors of $Ti_{75}Ni_{25}$ melts three independent measurements of total structure factors must be performed under different scattering contrast conditions. Neutron scattering together with isotopic substitution allows varying the scattering contrast. Therefore, we have performed neutron diffraction measurements on $Ti_{75}Ni_{25}$ alloy melts prepared with Ni of natural isotopic abundance (^{nat}Ni) and with the Ni isotopes ^{58}Ni and ^{60}Ni. An additional set of data was provided by x-ray diffraction on a sample prepared with ^{nat}Ni. The total structure factors determined by means of this at a temperature of $T = 1285$ K are shown in figure 1. For these different experiments on liquid $Ti_{75}Ni_{25}$ the pre-factors of the partial structure factors in equations (1) and (2) are listed in table 1 using values of the neutron scattering lengths from [29] and of the atomic x-ray scattering factors from [30].

Table 1. Weightings of the partial structure factors in the different measured total structure factors (A = Ti, B = Ni). For the case of x-ray diffraction, the values at $q = 2.75$ Å^{-1} are given, which corresponds roughly to the position of the first maximum of the total x-ray structure factor.

	$\frac{\bar{b}^2}{\overline{b^2}}$	$\frac{c_A c_B (b_A - b_B)^2}{\overline{b^2}}$	$\frac{2(b_A - b_B)\bar{b}}{\overline{b^2}}$	$\frac{c_A^2 b_A^2}{\overline{b^2}}$	$\frac{c_B^2 b_B^2}{\overline{b^2}}$	$\frac{2c_A c_B b_A b_B}{\overline{b^2}}$
$Ti_{75}{}^{nt}Ni_{25}$	≈0	≈1	≈0	0.188	0.187	−0.375
$Ti_{75}{}^{60}Ni_{25}$	0.326	0.674	−2.17	0.614	0.045	−0.333
$Ti_{75}{}^{58}Ni_{25}$	0.017	0.983	0.60	0.110	0.213	−0.306
$Ti_{75}Ni_{25}$ x-ray @2.75 Å^{-1}	0.977	0.023	0.69	0.457	0.098	0.423

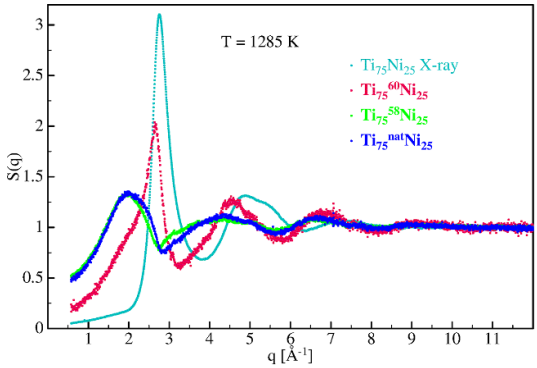

Figure 1. Total structure factors measured at 1285 K for liquid $Ti_{75}^{nat}Ni_{25}$, $Ti_{75}^{58}Ni_{25}$ and $Ti_{75}^{60}Ni_{25}$ by neutron diffraction and for liquid $Ti_{75}Ni_{25}$ by synchrotron x-ray diffraction.

While the neutron scattering lengths for nuclear scattering are independent of the scattering vector q, the atomic x-ray scattering factors decrease with increasing q. In table 1 we give the weightings of the partial structure factors in x-ray scattering experiments at a scattering vector of $q = 2.75$ Å^{-1}, which corresponds roughly to the position of the first maximum of the total x-ray structure factor. The q dependence of the scattering factors was taken into account when calculating the partial structure factors. Due to the negative coherent neutron scattering length of Ti ($b_{Ti} = -3.438$ fm) and the positive scattering length of Ni of natural isotopic abundance ($b_{natNi} = 10.3$ fm) the $Ti_{75}^{nat}Ni_{25}$ alloy corresponds nearly exactly to what is known as a zero-scattering alloy, for which $\bar{b} = c_A b_A + c_B b_B = 0$. Hence in eq. 1 the pre-factors of S_{NN} and S_{NC} are vanishing, while that of S_{CC} is 1 (see table 1). This means that the total structure factor measured for $Ti_{75}^{nat}Ni_{25}$ by neutron scattering corresponds to the partial structure factor S_{CC}. Only a small variation of the pre-factors of the partial structure factors is achieved when using the isotope ^{58}Ni instead of Ni of natural isotopic abundance (see table 1). Therefore, the corresponding total structure factors exhibit only small differences (see figure 1). Due to this poor scattering contrast, with the exception of S_{CC} and S_{NC}, comparatively large errors of the partial structure factors are expected, when calculating these from the three total structure factors measured by neutron scattering on $Ti_{75}^{nat}Ni_{25}$, $Ti_{75}^{58}Ni_{25}$, and $Ti_{75}^{60}Ni_{25}$. Significantly different contrast conditions, however, are obtained when using x-rays. As shown in table 1, for x-ray scattering the pre-factor of S_{NN} is close to 1, which means that the total x-ray structure factor can be considered as a reasonable approximation of S_{NN}.

Figure 2 shows a comparison between the partial structure factors at $T = 1285$ K calculated from the neutron diffraction data on liquid $Ti_{75}^{nat}Ni_{25}$, $Ti_{75}^{58}Ni_{25}$, and $Ti_{75}^{60}Ni_{25}$ (blue dots) and the partial structure factors calculated from the combination of the x-ray diffraction data and the neutron diffraction data on $Ti_{75}^{58}Ni_{25}$ and $Ti_{75}^{60}Ni_{25}$ (red dots). Both data sets reveal identical peak positions and identical peak amplitudes, within the experimental uncertainties. This confirms the reproducibility of the results obtained by the two different diffraction techniques (x-ray and neutron diffraction) in combination with electrostatic levitation. As expected in the light of the scattering contrast (see table 1) the partial structure factors obtained from the combination of the x-ray diffraction data and neutron diffraction data are less noisy.

Figure 3 shows the partial Bhatia–Thornton (upper panel) and Faber-Ziman (lower panel) structure factors determined from the diffraction measurements at 4 different temperatures (1150 K, 1285 K, 1410 K, and 1590 K). Please note that the measurements at 1150 K were performed within the metastable regime of an undercooled liquid below the liquidus temperature of $T_L = 1225$ K. The partial structure factors at 1285 K and 1410 K have been calculated from the x-ray diffraction measurements

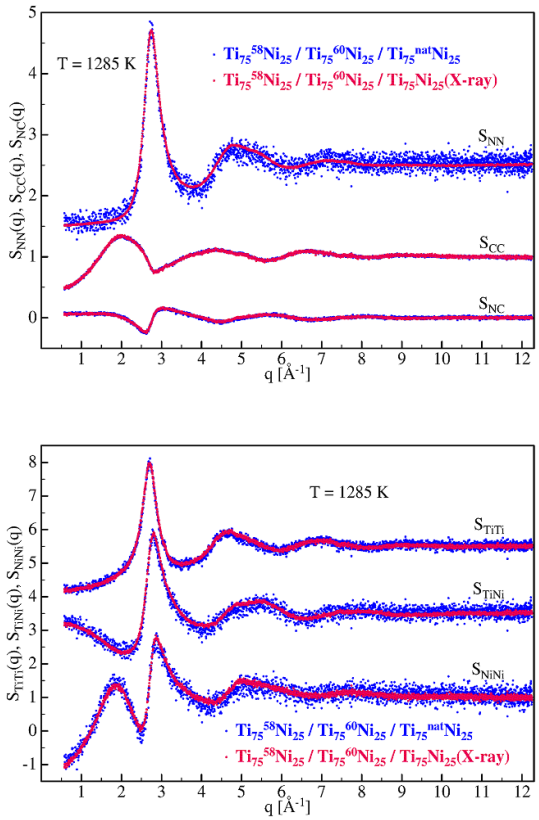

Figure 2. Comparison between the partial structure factors at $T = 1285$ K calculated from the neutron diffraction data on liquid $Ti_{75}^{nat}Ni_{25}$, $Ti_{75}^{58}Ni_{25}$, and $Ti_{75}^{60}Ni_{25}$ (blue dots) and the partial structure factors calculated from the combination of the x-ray diffraction data and the neutron diffraction data on $Ti_{75}^{58}Ni_{25}$ and $Ti_{75}^{60}Ni_{25}$ (red dots). In the upper part the partial Bhatia–Thornton structure factors, S_{NN}, S_{CC} and S_{NC}, are shown and in the lower part the partial Faber-Ziman structure factors, S_{TiTi}, S_{NiNi} and S_{TiNi}. For visualization, S_{NN}, S_{TiNi} and S_{TiTi} are shifted along the vertical axis. The good agreement of the data obtained by application of the different experimental techniques (solely neutron scattering with isotopic substitution and neutron scattering combined with x-ray diffraction) confirms the reproducibility of the experimental results.

and the neutron diffraction measurements on $Ti_{75}^{58}Ni_{25}$ and $Ti_{75}^{60}Ni_{25}$, which provides excellent contrast conditions. Unfortunately, due to an instability of the levitation, the $Ti_{75}^{60}Ni_{25}$ sample got lost before we were able to investigate this melt at the other temperatures. Therefore, the partial structure factors at 1150 K and 1590 K have been calculated from the x-ray data and the neutron data measured for $Ti_{75}^{58}Ni_{25}$ and $Ti_{75}^{nat}Ni_{25}$. The lower scattering contrast explains the larger noise of these structure factors. This is strongest at 1590 K where we were only able to acquire neutron scattering data on the $Ti_{75}^{58}Ni_{25}$ melt for 9 min (instead of typically 1–2 h) before the sample became unstable and got lost.

As observed also for many other metallic melts [10, 12, 13, 31–33], only gradual changes of the partial structure factors are observed as a function of the temperature, like an increase of the amplitudes of the oscillations or minor changes of the positions of the maxima when decreasing the temperature. No fundamental changes of the characteristic features of the structure factors are found in the investigated temperature regime, indicating that there are no drastic changes of the short-range structure. When comparing S_{CC} with the Faber-Ziman structure factors it can be seen that the first maximum of S_{CC} mainly results from the pre-peak of S_{NiNi}.

By a Fourier transformation of the Bhatia–Thornton partial structure factors (S_{NN}, S_{CC} and S_{NC}) and of the Faber-Ziman partial structure factors (S_{TiTi}, S_{NiNi} and S_{TiNi}), the partial Bhatia–Thornton pair correlation functions (g_{NN}, g_{CC} and g_{NC}) and the partial Faber-Ziman pair correlation functions (g_{TiTi}, g_{NiNi} and g_{TiNi}) were determined. These are plotted as a function of the temperature in figure 4.

g_{CC} shows a minimum at about 2.5 Å that is indicative of a chemical short-range order with a preference to form heterogeneous Ni–Ti nearest neighbor pairs in the melt. For a quantitative analysis of the melt structure, the nearest neighbor distances as well as the coordination numbers were extracted from the partial Bhatia–Thornton and Faber-Ziman pair correlation functions. The nearest neighbor distance d_{AB} corresponds to the position of the first maximum in g_{AB} (A,B = N, Ti, Ni). They are presented in table 2. The partial coordination numbers Z_{AB} are calculated by integrating the first maximum of the partial radial distribution function $4\pi c_B \rho_N r^2 g_{AB}(r)$ (A,B = N, Ti, Ni) between its first and second

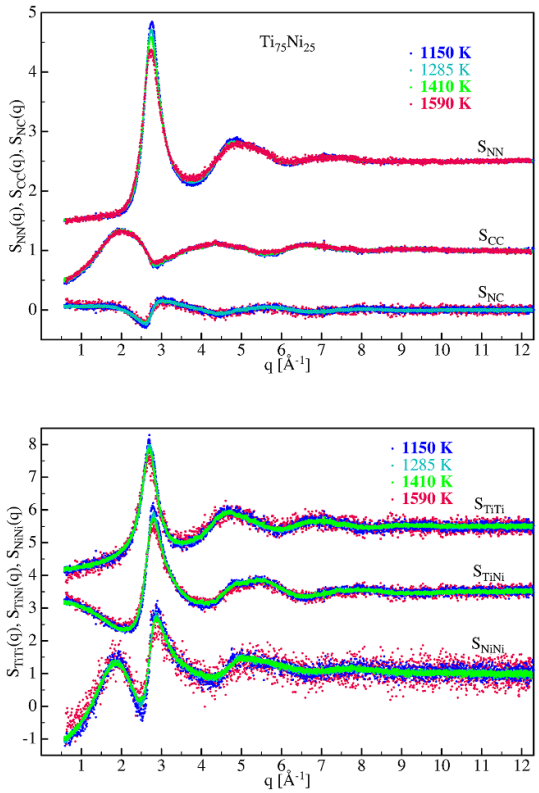

Figure 3. Partial Bhatia–Thornton structure factors, S_{NN}, S_{CC} and S_{NC} (upper part), and partial Faber-Ziman structure factors, S_{TiTi}, S_{NiNi} and S_{TiNi} (lower part), of $Ti_{75}Ni_{25}$ melts at different temperatures. For visualization, S_{NN}, S_{TiNi} and S_{TiTi} are shifted along the vertical axis.

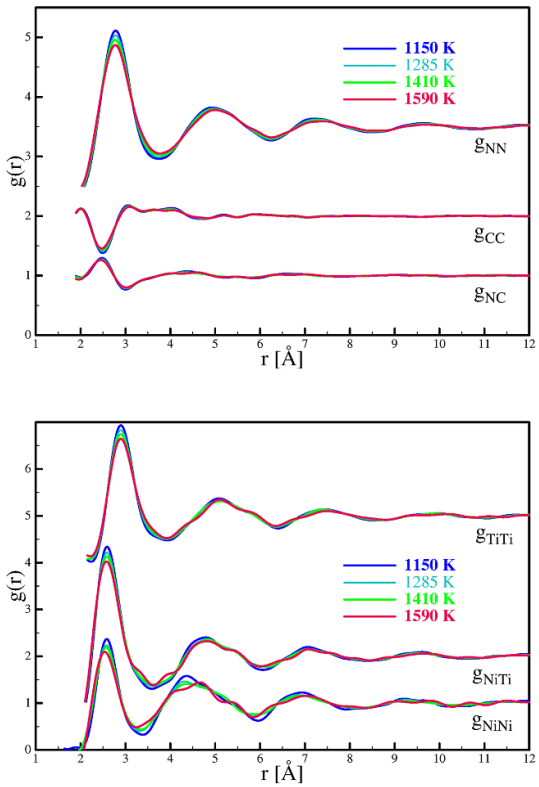

Figure 4. Partial Bhatia–Thornton pair correlation functions, g_{NN}, g_{CC} and g_{NC} (upper part), and partial Faber-Ziman pair correlation functions, g_{TiTi}, g_{NiNi} and g_{TiNi} (lower part), of $Ti_{75}Ni_{25}$ melts at different temperatures. For visualization, the curves are shifted along the vertical axis.

Table 2. Nearest neighbor distances d_{NN}, d_{NiNi} d_{TiTi}, and d_{TiNi} in liquid $Ti_{75}Ni_{25}$ at different temperatures.

T (K)	d_{NN} (Å)	d_{NiNi} (Å)	d_{TiTi} (Å)	d_{TiNi} (Å)
1590	2.77 ± 0.02	2.54 ± 0.04	2.90 ± 0.03	2.57 ± 0.03
1410	2.77 ± 0.02	2.57 ± 0.02	2.89 ± 0.02	2.58 ± 0.02
1285	2.78 ± 0.02	2.57 ± 0.02	2.89 ± 0.02	2.59 ± 0.02
1150	2.78 ± 0.02	2.58 ± 0.02	2.90 ± 0.02	2.59 ± 0.02

Table 3. Partial nearest neighbor coordination numbers (Z_{NN}, Z_{NiNi}, Z_{TiTi}, Z_{NiTi}, Z_{TiNi}), average coordination number $\langle Z\rangle$ and coordination numbers of the Ti and Ni atoms (Z_{Ti} and Z_{Ni}) for melts of $Ti_{75}Ni_{25}$ at different temperatures. The error of the coordination numbers amounts to ± 0.5.

T (K)	Z_{NN}	$\langle Z\rangle$	Z_{NiNi}	Z_{TiTi}	Z_{TiNi}	Z_{NiTi}	Z_{Ni}	Z_{Ti}
1590	13.4	13.7	1.8	11.3	9.5	3.2	11.3	14.5
1410	13.3	13.7	2.0	11.3	9.6	3.2	11.5	14.5
1285	13.5	13.8	2.0	11.3	9.6	3.2	11.6	14.5
1150	13.5	14.0	2.0	11.5	9.7	3.2	11.8	14.7

minimum. Here ρ_N denotes the number density that is calculated from measured values of the density of liquid $Ti_{75}Ni_{25}$ provided in [15]. The partial coordination numbers are compiled in table 3.

The interatomic distance d_{NiTi} is smaller compared to $(d_{NiNi} + d_{TiTi})/2$ at all temperatures (see table 2), which is an indication for strong interactions between the atoms of Ni and Ti. Furthermore, d_{NiTi} is also smaller than the sum of the Goldschmidt radii of Ni ($r_{Ni,GS} = 1.24$ Å [34]) and Ti ($r_{Ti,GS} = 1.47$ Å [34]), or half of the sum of the nearest neighbor distances $(d_{Ti} + d_{Ni})/2$ in pure liquid Ti ($d_{Ti} = 2.86$ Å) [32] and Ni ($d_{Ni} = 2.49$ Å) [31]. While in melts of pure Ni the nearest neighbor distance $d_{NiNi} = 2.49$ Å corresponds to twice of the Goldschmidt radius, the Ni–Ni nearest neighbor distances in liquid $Ti_{75}Ni_{25}$ are larger by about 3%. (when taking the more precise values measured at the lower and intermediate temperatures). While a contraction of the Ti–Ni nearest neighbor distances and a widening of the Ni–Ni distances is observed in in liquid $Ti_{75}Ni_{25}$ no such effect is found for d_{TiTi} (the values are between the nearest neighbor distances in liquid Ti and twice of the Goldschmidt radius). Similar contractions or expansions of the nearest neighbor distances were reported for melts of Zr–Ni alloys [10, 12], $Hf_{35}Ni_{65}$ [12], and $Ni_{66.7}B_{33.3}$ [13]. Also for these melts the formation of nearest neighbor pairs consisting of unlike atoms is preferred.

The nearest neighbor coordination number Z_{NN} that is calculated from the Bhatia–Thornton structure factor S_{NN}, is in good agreement with the mean coordination number $\langle Z\rangle = c_{Ti}(Z_{TiTi} + Z_{NiTi}) + c_{Ni}(Z_{NiNi} + Z_{TiNi})$ that is determined from the Faber-Ziman partial structure factors (see table 3). The minor deviation is due to the errors in the determination of the different partial coordination numbers (including those due to the Fourier transformation when calculating the pair correlation functions from the structure factors).

Like for binary $Zr_{64}Ni_{36}$ melts [7], a large nearest neighbor coordination number $Z_{NN} > 13$ prevails in binary $Ti_{75}Ni_{25}$ melts. This indicates a dense local packing. Such large coordination numbers are incompatible with a dominating icosahedral short-range order that is characterized by coordination numbers of 12. The coordination numbers of the larger Ti atoms $Z_{Ti} = Z_{TiTi} + Z_{NiTi}$ are considerably higher than those of the smaller Ni atoms $Z_{Ni} = Z_{NiNi} + Z_{TiNi}$, indicating different environments of the atomic species. For a further analysis of the chemical order the Warren Cowley [35] order parameters defined by $\alpha^1{}_{AB} = 1—Z_{BA}/(Z_A\, c_B)$ were calculated. If the concentration of B atoms in the first coordination shell around an A atom, Z_{BA}/Z_A, is larger than the overall concentration of B atoms in the melt, c_B, then $\alpha^1{}_{AB} < 0$, if it is smaller than c_B then $\alpha^1{}_{AB} > 0$. For liquid $Ti_{75}Ni_{25}$ we find $\alpha^1{}_{TiNi} \approx 0.1$ and $\alpha^1{}_{NiTi} \approx -0.1$. This means that the first coordination shell around the Ni atoms is enriched with Ti, while the first coordination shell around the Ti atoms is depleted of Ni. For an analysis of the overall chemical short-range oder Cargill-Spaepen order parameter [36] can be calculated $\eta^{CS} = Z_{NiTi}\, \langle Z\rangle/(c_{Ni}\, Z_{Ni}\, Z_{Ti})–1 \approx 0.05$. Its slightly positive value points to some preference for the formation of heterogeneous Ni–Ti nearest neigbor pairs.

Figure 5 shows the mean Ti/Ni self-diffusion coefficients in $Ti_{75}Ni_{25}$ melts as a function of the inverse temperature as measured in an earlier investigation [15] by quasielastic neutron scattering. Within the investigated temperature range the self-diffusion coefficients show an Arrhenius-type temperature dependence with an activation energy of $E_a = 0.56$ eV [15].

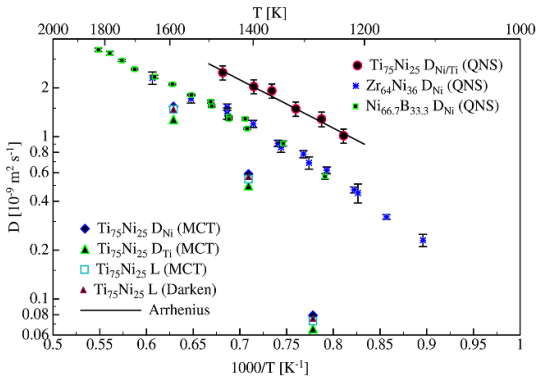

Figure 5. Mean Ni/Ti self-diffusion coefficients determined for liquid $Ti_{75}Ni_{25}$ by quasielastic neutron scattering [15] (red circles), Ni (blue diamonds) and Ti (green triangles) self-diffusion coefficients calculated in the framework of the mode coupling theory, Onsager coefficients calculated within the mode coupling theory (cyan squares) and from the self-diffusion coefficients by use of Darken's equation (pink triangles). The black line is an Arrhenius fit to the experimentally measured Ni/Ti self-diffusivities. Also shown are the Ni self-diffusion coefficients of liquid $Zr_{64}Ni_{36}$ [7, 20] (blue stars) and $Ni_{66.7}B_{33.3}$ [14] (green squares).

The MCT of the glass transition [5] establishes a firm relationship between the short-range order and dynamic properties of the melt like self-diffusion coefficients or viscosity. The only input parameters of MCT calculations are partial static structure factors and packing densities. Although MCT was originally developed to describe the glass transition, it is really a theory of structural relaxation in the moderately viscous fluid. Comparison to experiment and computer simulation clearly demonstrates that MCT describes the first three to four orders of magnitude in slowing down compared to the high-temperature fluid [5]. Our data fall into this regime. While MCT is known to frequently underestimate the absolute values of the transport coefficients, especially at temperatures close to the critical temperature, MCT is typically able to capture the interrelations between the transport coefficients, such as the ratio of the self-diffusion coefficients, well [6, 8]. We have calculated the Ni and Ti self-diffusion coefficients in the framework of the MCT using the partial Faber-Ziman structure factors of figure 3 as an input (for details of the procedure, see [8, 13] and references therein). While the Ti and Ni self-diffusion coefficients calculated by the MCT at the highest temperature (1590 K) underestimates the experimentally determined mean Ti/Ni self-diffusion coefficients at similar temperatures by roughly a factor of three, when decreasing the temperature, a much stronger decrease of the diffusivities is suggested by MCT as experimentally observed (see figure 5). This may indicate the closeness to the critical temperature T_C of MCT. Because of this divergence the attempt to calculate diffusion coefficients from the partial structure factors by MCT even failed at the lowest temperature (1150 K). However, it must be considered that the temperature is an indirect parameter in MCT calculations, since the slowing down in the dynamics is mostly driven by temperature-induced changes of the density-correlation functions. While the temperature dependence itself is incorrect, one expects MCT to capture the interrelations between the transport coefficients well.

At all the three temperatures at which MCT calculations were possible the MCT suggest that the Ni self-diffusion is slightly faster than the Ti self-diffusion with a ratio of $D_{Ni}/D_{Ti} \approx 1.2$. The small deviation of this ratio from 1 (full coupling) indicates pronounced coupling of the Ni and Ti self-diffusion. This may be a result of strong chemical interactions between Ni and Ti which is supported by the observed shortening of the Ni–Ti interatomic distances. The small difference of the self-diffusion coefficients also justifies the determination of a mean Ni/Ti self-diffusion coefficient from quasielastic neutron scattering experiments [15]. The interdiffusion coefficient D_{int} is the product of the Onsager coefficient L and the thermodynamic factor Φ: $D_{int} = \Phi L$. The Onsager coefficients L calculated by MCT are in good agreement with those suggested by Darken's equation ($L_D = c_{Ni}{}^*D_{Ti} + c_{Ti}{}^*D_{Ni}$) [37]. This shows that cross-correlation effects are negligible for liquid $Ti_{75}Ni_{25}$. While some characteristics like the contraction of the distances of unlike nearest neighbors, the large coordination numbers or the comparatively strong coupling of the self-diffusion coefficients are similar in $Ti_{75}Ni_{25}$ and $Zr_{64}Ni_{36}$ melts, the interdiffusion behavior in both liquids is obviously different (for $Zr_{64}Ni_{36}$. Darken's equation is not valid [8, 11]). On the other hand, for melts of $Ni_{66.7}B_{33.3}$ the MCT calculations suggest decoupled dynamics of the constituents (B diffuses roughly twice as fast as Ni) and that, similar as for $Ti_{75}Ni_{25}$, the interdiffusion is well described by Darken's equation [13].

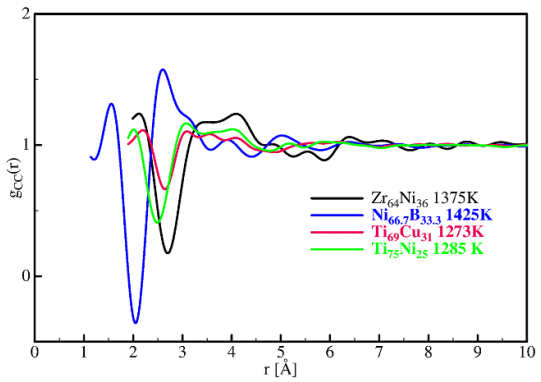

Figure 6. Partial Bhatia–Thornton pair correlation functions g_{CC} for liquid $Ti_{75}Ni_{25}$, $Zr_{64}Ni_{36}$ [7], $Ti_{69}Cu_{31}$ [17], and $Ni_{66.7}B_{33.3}$ [13].

One parameter, amongst others, that is considered to strongly influence the atomic mobility in liquid metals is the packing fraction [38]. Melts of $Ti_{75}Ni_{25}$, $Ti_{69}Cu_{31}$, $Zr_{64}Ni_{36}$ and $Ni_{66.7}B_{33}$ are consisting of a larger atomic species as the majority component and a smaller atomic species as the minority component. All these alloys melts are characterized by similar packing fractions ranging from 0.52 ($Ni_{66.7}B_{33}$) to 0.55 ($Zr_{64}Ni_{36}$) at $T = 1273$ K [14–17]. With the exception of the metal-metalloid alloy $Ni_{66.7}B_{33}$, they can be considered as chemically similar alloys, consisting of a group 4 element (Ti, Zr) and a late transition metal (Ni, Cu). While the Ni self-diffusion coefficients of liquid $Zr_{64}Ni_{36}$ [7, 20] and $Ni_{66.7}B_{33.3}$ [14] are similar at same temperatures, $Ti_{75}Ni_{25}$ shows higher mean Ni/Ti self-diffusion coefficients [15] (see figure 5). A similar behavior is found for the collective dynamics. While melts of $Zr_{64}Ni_{36}$ [16] and $Ni_{66.7}B_{33.3}$ [14] show similar viscosities at same temperatures, liquid $Ti_{75}Ni_{25}$ [15] and even more so $Ti_{69}Cu_{31}$ [17] are characterized by faster dynamics. In order to find a possible structural explanation for these differences in the atomic dynamics, we have a closer look on the chemical short-range order of the melts that is described by the Bhatia–Thornton partial pair correlation functions g_{CC}. These are depicted in figure 6 for the different alloy melts. In all cases a minimum of g_{CC} is found that is characteristic for a chemical short-range order with a preference for the formation of heterogeneous nearest neighbor pairs. Nevertheless, the depth of the minima is smallest for both Ti-based melts, with $Ti_{69}Cu_{31}$ showing the lowest depth. This indicates that the chemical short-range order is less pronounced for the Ti-based melts which may provide an explanation for the faster atomic dynamics. This is in good agreement with results of first-principles based molecular-dynamics simulations on Ti–Cu melts that indicate comparatively weak Ti–Cu interactions [39]. MCT predicts Ni and Ti self-diffusion on the basis of the partial static structure factors (in the Faber-Ziman nomenclature): a pronounced $S_{TiNi}(q)$ gives rise to a strong coupling between the species. In this sense, the degree of the chemical interaction described through $S_{CC}(q)$ (figure 6) can be linked to the strength of the coupling of the self-diffusion coefficients, although $S_{CC}(q)$ itself does not directly enter MCT.

4. Conclusions

We have determined partial structure factors of liquid $Ti_{75}Ni_{25}$ alloys by a combination of neutron diffraction (with isotopic substitution) and synchrotron x-ray diffraction. The studies reveal that $Ti_{75}Ni_{25}$ melts are characterized by a chemical short-range order, where heterogeneous Ti–Ni nearest neighbors are preferentially formed. This chemical short-range order, however, is less pronounced than the chemical short-range order reported for melts of $Zr_{64}Ni_{36}$ [7] and $Ni_{66.7}B_{33.3}$ [13]. The less pronounced chemical short-range order may account for the faster atomic dynamics reported for liquid $Ti_{75}Ni_{25}$ as compared to that of molten $Zr_{64}Ni_{36}$ or $Ni_{66.7}B_{33.3}$, which are characterized by similar packing fractions. An analysis of the structure-dynamics relationship in the framework of the MCT of the glass transition suggest that the Ni self-diffusion is slightly faster than the Ti self-diffusion with a ratio of $D_{Ni}/D_{Ti} \approx 1.2$. Moreover, the Onsager coefficients calculated by MCT are in good agreement with those estimated by use of Darken's equation indicating that for liquid $Ti_{75}Ni_{25}$ cross-correlation effects are negligible. This is different for molten $Zr_{64}Ni_{36}$, where Darken's equation is not valid,

Acknowledgments

We acknowledge M. Frey, B. Adam and S. Szabó for their assistance during the D20 beamtime and E. Sondermann for carefully reviewing the manuscript. For financial support, we gratefully acknowledge the German Research Foundation (DFG) through the grants No. ME 1958/12-1 and BU 2276/11-1.

Data availability statement

The data cannot be made publicly available upon publication because the cost of preparing, depositing and hosting the data would be prohibitive within the terms of this research project. The data that support the findings of this study are available upon reasonable request from the authors.

ORCID iDs

Dirk Holland-Moritz 0009-0000-2457-7427
Fan Yang 0000-0001-5281-2957
Nico Neuber 0000-0002-9912-5764
Ralf Busch 0000-0002-1696-271X
Thomas Voigtmann 0000-0002-1261-9295
Andreas Meyer 0000-0002-0604-5467

References

[1] Kelton K F 2022 Theory of nucleation and glass formation *Metallurgy in Space (The Minerals, Metals & Materials Series)* ed Fecht H J and M Mohr (Springer)
[2] Herlach D M *et al* 2014 *Metals* **4** 196
[3] Asta M, Beckermann C, Karma A, Kurz W, Napolitano R, Plapp M, Purdy G, Rappaz M and Trivedi R 2009 *Acta Mater.* **57** 941
[4] Kurz W *et al* 1992 *Fundamentals of Solidification* 3rd edn (Trans Tech Publications, Aedermannsdorf)
[5] Götze W 2008 *Complex Dynamics of Glass-Forming Liquids: A Mode-Coupling Theory* vol 143 (Oxford University Press)
[6] Götze W and Sjogren L 1992 *Rep. Prog. Phys.* **55** 241
[7] Holland-Moritz D, Stüber S, Hartmann H, Unruh T, Hansen T and Meyer A 2009 *Phys. Rev. B* **79** 064204
[8] Voigtmann T, Meyer A, Holland-Moritz D, Stüber S, Hansen T and Unruh T 2008 *Europhys. Lett.* **82** 66001
[9] Basuki S W et al 2017 *Phys. Rev. B* **95** 024301
[10] Nowak B, Holland-Moritz D, Yang F, Voigtmann T, Kordel T, Hansen T C and Meyer A 2017 *Phys. Rev. Mater.* **1** 025603
[11] Yang F, Heintzmann P, Kargl F, Binder K, Nowak B, Schillinger B, Voigtmann T and Meyer A 2018 *Phys. Rev. B* **98** 064202
[12] Nowak B, Holland-Moritz D, Yang F, Voigtmann T, Evenson Z, Hansen T C and Meyer A 2017 *PRB* **96** 054201
[13] Nell S, Yang F, Holland-Moritz D, Voigtmann T, Hu J, Hansen T C, Buslaps T and Meyer A 2024 *Phys. Rev. B* **110** 014206
[14] Nell S, Yang F, Evenson Z and Meyer A 2021 *Phys. Rev. B* **103** 064206
[15] Wilden J, Yang F, Holland-Moritz D, Szabó S, Lohstroh W, Bochtler B, Busch R and Meyer A 2020 *Appl. Phys. Lett.* **117** 013702
[16] Brillo J, Pommrich A I and Meyer A 2011 *Phys. Rev. Lett.* **107** 165902
[17] Kreuzer L P, Yang F, Evenson Z, Holland-Moritz D, Bernasconi A, Hansen T C, Blankenburg M, Meyer A and Petry W 2024 *Phys. Rev. B* **109** 174108
[18] Bhatia A B and Thornton D E 1970 *Phys. Rev. B* **2** 3004
[19] Faber T E and Ziman J M 1965 *Phil. Mag.* **11** 153
[20] Kordel T, Holland-Moritz D, Yang F, Peters J, Unruh T, Hansen T and Meyer A 2011 *Phys. Rev. B* **83** 104205
[21] Nash P 1991 *Phase Diagrams of Binary Nickel Alloys* (ASM International)
[22] Wilden J *et al* 2020 *Impact of Sulfur on the Structure and Dynamics of Glass-forming Metallic Melts* Institut Laue-Langevin (ILL) (https://doi.org/10.5291/ILL-DATA.6-05-1011)
[23] Hansen T C, Henry P F, Fischer H E, Torregrossa J and Convert P 2008 *Meas. Sci. Technol.* **19** 034001
[24] Holland-Moritz D et al 2005 *Meas. Sci. Technol.* **16** 372
[25] Bernasconi A, Wright J and Harker N 2015 *Powder Diffr.* **30** S2
[26] Labiche J-C, Mathon O, Pascarelli S, Newton M A, Ferre G G, Curfs C, Vaughan G, Homs A and Carreiras D F 2007 *Rev. Sci. Instrum.* **78** 091301
[27] Kieffer J, Valls V, Blanc N and Hennig C 2020 *J. Synchrotron Radiat.* **27** 558
[28] Qiu X, Thompson J W and Billinge S J L 2004 *J. Appl. Crystal.* **37** 678
[29] Sears V F 1992 *Neutron News* **3** 29
[30] Cromer D T *et al* 1974 *International Tables for Crystallography* vol 4 (Kynoch Press)
[31] Schenk T et al 2002 *Phys. Rev. Lett.* **89** 075507
[32] Holland-Moritz D, Heinen O, Bellissent R and Schenk T 2007 *Mater. Sci. Eng. A* **449–451** 42
[33] Dai R, Neuefeind J C, Quirinale D G and Kelton K F 2020 *J. Chem. Phys.* **152** 164503
[34] Pauling L 1947 *J. Am. Chem. Soc.* **69** 542
[35] Cowley J M 1950 *Phys. Rev.* **77** 669
[36] Cargill I I I G S and Spaepen F 1981 *J. Non-Cryst. Solids* **43** 9
[37] Darken L S 1948 *Trans AIME* **175** 184
[38] Takeuchi A and Inoue A 2005 *Mater. Trans.* **46** 2817
[39] Kreuzer L P, Yang F, Meyer A and Jakse N 2025 *Phys. Rev. B* **111** 144107